

Coupled Assessment of Landscape Quality and Vitality in Historic Districts: A Multi-Source Street-Level Study of Xiwenmiaoping, Changsha

Yanxiang Wang, Jing Li*

School of Architecture and Art, North China University of Technology, Beijing, China

**Corresponding Author*

Abstract: This study addresses the lack of systematic quantitative analysis in historic district revitalization by examining the Xiweng Miping Historic District in Changsha. A three-dimensional framework was developed, comprising the Facade Quality Index (FQI), Service Attractiveness Index (SGI), and Activity Vitality Index (AVI), integrating deep learning street scene analysis, multi-source POI data, social media, and YOLOv8-based pedestrian detection. Quantitative assessment and K-means clustering of 32 street segments reveal a negative correlation between FQI and AVI ($r = -0.390$, $p = 0.024$), indicating that physical restoration alone does not enhance vitality. Misaligned cultural and commercial POIs further limit functional transformation into vitality. Four coupling types were identified, with the “comprehensive low-value” type dominant (40.6%), reflecting limited revitalization efficiency. Findings suggest that improving vitality requires coordinated planning of cultural and commercial projects and better accessibility, offering evidence-based support for refined historic district renewal.

Keywords: Historic District; Street-View Imagery; Deep Learning; Spatial Vitality; Coupling Analysis

1. Introduction

As China’s urbanization shifts from incremental expansion to the renewal of existing stock, urban renewal has become a central focus of planning efforts. As key repositories of urban cultural memory, historic and cultural districts have been elevated to a strategic priority for protection and revitalization at the national level [1]. In 2024, the Ministry of Housing and Urban-Rural Development explicitly required that the protection of historical and cultural heritage be

integrated throughout the entire urban renewal process, and established rigorous and detailed quality assessments as a prerequisite for advancing from physical preservation to the transmission of cultural values.

Existing quantitative studies on environmental quality primarily rely on case studies, questionnaires, and expert ratings [2–5]; these methods are inherently subjective and unsuitable for large-scale, detailed assessments [6]. In recent years, the integration of street-view imagery with deep learning has opened up new avenues of research [7–9]: researchers have used computer vision to extract objective indicators such as the “Green View Index” (GVI) and the “Sky View Factor” (SVF) [10], and have leveraged machine learning to predict public perception, thereby significantly improving assessment efficiency and spatial resolution. Some studies have attempted to establish a correlation between the historical characteristics of building facades and perceived street quality [11, 12]. However, such research is primarily limited to the neighborhood level, lacking systematic quantification at the finer street segment level, and the various dimensions of environmental factors have not yet been systematically integrated. On the other hand, pedestrian traffic measurements based on object detection [13] and user-generated content (UGC) data [14] provide effective approaches for assessing vitality; however, existing studies often employ these methods in isolation. Research that systematically integrates both and analyzes their coupling with spatial quality remains rare, and this critical question of whether a spatial mismatch exists between quality and vitality has not yet been fully explored at the street segment scale.

In summary, there are three major gaps in the existing literature. First, quality assessments of historic districts primarily focus on the district as a whole, making it difficult to identify

differences in quality among individual street segments within the district. Second, the three dimensions—physical environment quality, spatial perceived attractiveness, and pedestrian behavior patterns—are treated as relatively independent, and there is a lack of a unified analytical framework for coupled analysis. Third, the relationship between quality and vitality lacks empirical validation at a fine-grained scale, making it difficult to implement renewal strategies with precision.

Based on this, this study takes the Xuwenmiao Ping Historic District in Changsha as a case study and focuses on two core questions: How do different sections of the district exhibit spatial differentiation across three dimensions—physical environmental quality, spatial perceptual attractiveness, and behavioral activity levels? Do these three dimensions exhibit a coupled or decoupled relationship, and what insights do their spatial patterns offer for differentiated revitalization strategies? To address these questions, a three-dimensional coupled evaluation framework—comprising the “physical layer, perceptual layer, and behavioral layer”—was developed. Cluster analysis was used to identify the types of spatial coupling among road segments, providing evidence-based support for differentiated revitalization strategies. The study’s innovations are reflected in three aspects: first, by using intersections as boundaries, the assessment granularity is refined to the street segment level; second, environmental quality, spatial attractiveness, and

human behavior are integrated into a unified analytical framework to construct a three-dimensional coupled model; and third, a behavioral-layer assessment method combining actual pedestrian flow data with social media data is adopted to enhance the comprehensiveness and robustness of vitality measurements.

2. Study Area

As the birthplace of Huxiang culture and a nationally designated historical and cultural city, Changsha’s organic renewal of its old city must balance the preservation of cultural heritage with functional restructuring. This study focuses on the Xiwenmiaoping Historic District in Tianxin District Figure 1, located in the southwestern part of ancient Changsha. The district embodies a millennium-old academic tradition, with a study area of approximately 34 km² and a fabric spanning from the Ming and Qing dynasties to the early years of the People’s Republic of China, characterized by temporal layering and spatial heterogeneity. However, its evolution toward “high density and low quality” has trapped it in a dual dilemma: constrained by the requirement to preserve authenticity, yet plagued by deteriorating infrastructure and poor environmental quality, it fails to live up to its lofty status as the “origin of Changsha.” The current approach is shifting from physical restoration to the targeted revitalization of the area.

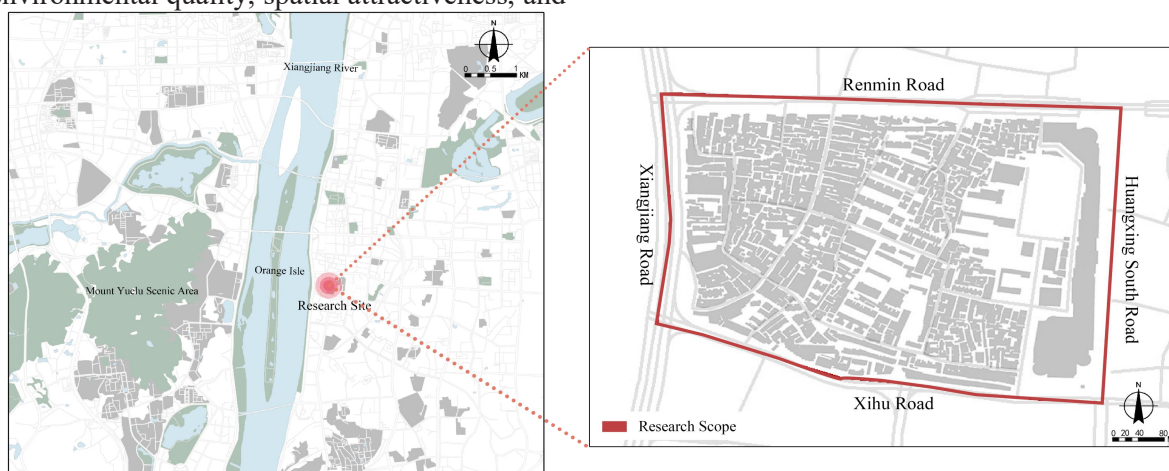


Figure 1. Geographical Location and Scope of the Study Area

3. Data and Methods

3.1 Data Collection and Preprocessing

3.1.1 Street-view imagery

In March 2026, the research team conducted systematic panoramic image acquisition across all road sections in the study area, incorporating both habitat perception and vitality measurement functions. For habitat perception, the

DeepLabv3+ semantic segmentation model was used to automatically extract the Green Viewing Index (GVI) and Sky Viewing Fraction (SVF) for each road section, with the average of all sampling points within each section taken as the representative value [15,16]; For pedestrian traffic, data collection was limited to the daily peak hours of 16:00–19:00. The YOLOv8 object detection model was employed for automatic pedestrian recognition and counting [17]. Following manual verification, the recognition accuracy was 80%. The measured pedestrian density (PDI, people/meter) was calculated by dividing the total number of pedestrians on each section by the section's length.

3.1.2 Building footprint data

Based on the publicly released draft of the Changsha Historic City Conservation Plan (2025–2035) and supplemented by field surveys, street-facing building facades along each segment were classified into three categories: traditional historic buildings (TH), historicist replica buildings (FH), and modern buildings (NH). Each category was further assessed across two dimensions—physical integrity and cultural authenticity—and rated at three quality levels (high, medium, low), yielding a dataset of 9 sub-indicator categories (3 types×3 quality levels).

3.1.3 Points of interest (POI) data

Using AutoNavi Maps and Baidu Maps as the primary data sources [18], and after conducting on-site verification and removing invalid entries, the data was categorized into three groups: cultural and historical sites, commercial services, and public facilities. The density per unit length

of these three types of POIs within the buffer zones of each road segment was then calculated.

3.1.4 Social media data

Social media data is used to characterize the degree of purposeful attention tourists pay to street spaces [19, 20]. By scraping content from Xiaohongshu and Douyin platforms between January 2025 and March 2026 that includes the keywords “Xiwénmiàopíng” and “Changsha Xiwenmiao Ping Historic District” between January 2025 and March 2026. Valid images were retained only if they featured street spaces as the primary subject and accounted for at least 40% of the frame. Based on spatial cues and posting locations, these images were matched to specific street segments. The check-in heat density (CHI, times/meter) was calculated by dividing the number of valid check-ins by the length of the street segment.

3.2 Methods

3.2.1 Spatial analysis unit delineation



Figure 2. Street and Alley Division Map

Table 1. Road Name and Numbering

Segment Code	Road Name	Segment Code	Road Name
<i>XWJ-3</i>	Xiuwen Street-3	QSJ-1	Quansijing-1
<i>TJWX-1</i>	Tangjiawan Lane-1	XWMP-1	Xiwenmiaoping-1
<i>DCYX-1</i>	Douchiyuan Lane-1	RMV-1	Renmeiyuan-1
<i>SJW-1</i>	Shijingwan-1	GLJP-1	Gongluju Ping-1
<i>XLJP-1</i>	Xia Lijia Slope-1	LDXC-1	Laodong Xincun-1
<i>XWJ-1</i>	Xiuwen Street-1	RMXL-2	Renmin West Road-2
<i>XYX-1</i>	Xueyuan Lane-1	LDXC-2	Laodong Xincun-2
<i>NQW-1</i>	Nanqiangwan-1	XJDD-1	Xiangjiang Avenue-1
<i>XHL-2</i>	Xihu Road-2	DRQX-1	Dengrenqiao Lane-1
<i>SLJP-1</i>	Shang Lijia Slope-1	XYJ-1	Xueyuan Street-1
<i>XWJ-2</i>	Xiuwen Street-2	RMXL-1	Renmin West Road-1
<i>GTJ-1</i>	Gutan Street-1	BHCX-1	Baihuacun Lane-1
<i>CJJ-1</i>	Chenjia Well-1	XJDD-2	Xiangjiang Avenue-2
<i>XGMZJ-1</i>	Xuegongmen Main Street-1	XWMP-2	Xiwenmiaoping-2
<i>BHX-1</i>	Baihe Lane-1	RMXL-3	Renmin West Road-3
<i>HXNL-1</i>	Huangxing South Road-1	XHL-1	Xihu Road-1

Given the complex spatial structure of historic districts—characterized by high building density and variable alley scales—conventional district-wide assessment units are inadequate for revealing intra-district spatial differentiation. This study adopts individual streets and alleys as the basic spatial analysis units. The entire alley system of Xiwenmiaoping was systematically inventoried and coded, yielding 32 street segment units (e.g., XWJ-1, TJWX-1, DCYX-1). Precise lengths were recorded through field measurement, serving as the spatial baseline for subsequent per-meter normalization Figure 2, Table 1.

3.2.2 Three-dimensional assessment framework

In terms of data integration logic, this study constructs a "physical layer–perceptual layer–behavioral layer" three-dimensional data framework, corresponding respectively to building facade quality [21], spatial gravity intensity [22], and pedestrian activity vitality. All three data types are spatially indexed to individual street segments, forming a unified multi-attribute data table that ensures both spatial comparability and analytical systematicity.

The Facade Quality Index (FQI) was derived using the Analytic Hierarchy Process (AHP) to assign weights to the 9 building sub-indicator categories [23], guided by the principles of historical authenticity and facade integrity. TH-HQ (traditional historic, high quality) received the highest weight (0.312), while NH-LQ (modern, low quality) received the lowest (0.027); the consistency ratio $CR < 0.1$,

Table 2. Building Quality Grades

Indicator	TH-HQ	TH-MQ	TH-LQ	FH-HQ	FH-MQ	FH-LQ	NH-HQ	NH-MQ	NH-LQ
<i>Weight</i>	0.312	0.208	0.087	0.208	0.064	0.038	0.087	0.042	0.027
<i>Rank</i>	1	2	4	3	6	8	5	7	9

Table 3. Weights of Spatial Gravity Indicators

Indicator	GVI	SVF	Cultural–Historical	Commercial–Service	Public Facility
<i>Weight</i>	0.067	0.333	0.335	0.192	0.073
<i>Rank</i>	5	2	1	3	4

Building on the three-dimensional normalized scores, the optimal number of clusters was determined by jointly applying the elbow method and silhouette coefficient. A K-means clustering algorithm was then used to classify the 32 street segments into coupling typologies [25]. The analysis confirmed $k = 4$ as the optimal cluster number, yielding four distinct spatial coupling patterns.

4. Results and Analysis

confirming acceptable consistency Table 2.

The Spatial Gravity Index (SGI) integrates five indicators: GVI, SVF, cultural–historical POI density, commercial–service POI density, and public facility POI density Table 3. Following AHP weighting, cultural–historical facilities (0.335) and spatial enclosure (SVF, 0.333) received the highest weights; $CR < 0.1$.

The Activity Vitality Index (AVI) synthesizes empirically measured pedestrian density and online check-in heat, weighted at 0.75 and 0.25 respectively based on AHP analysis, reflecting the greater objectivity of empirically measured behavioral data relative to network perception data.

To eliminate the confounding effect of absolute quantity differences arising from varying segment lengths, all indicators were first aggregated at the segment level and then converted to per-linear-meter means, before being AHP-weighted and normalized for inclusion in the composite assessment model. This ensures cross-dimensional and cross-unit comparability.

3.2.3 Normalization and coupling analysis

To examine the degree of statistical association among the physical, perceptual, and behavioral dimensions, FQI, SGI, and AVI scores were uniformly subjected to Min-Max normalization, mapped to the [0, 1] interval. Spearman rank correlation analysis was applied to all three pairwise dimensional combinations [24] ($n = 32$, $\alpha = 0.05$) to determine whether synergistic reinforcement or structural divergence exists between dimensions.

4.1 Spatial Heterogeneity of Building Facade Quality

The architectural facade quality along different sections of the Xuwen Miaoping Historic District exhibits significant spatial variation, generally following a concentric pattern of decline from the district's historic core toward its outer boundaries Figure 3. The differences in normalized scores for the architectural character of each section are substantial, indicating a high

degree of spatial variation.

From a spatial distribution perspective, there is a marked disparity in quality between the internal alleys of the neighborhood and the surrounding arterial roads. Along the internal alleys, the density of historic buildings is relatively high, the continuity of facade styles is strong, and the streetscape as a whole exhibits a high degree of historical legibility and physical integrity; in contrast, the sections bordering the city's main

thoroughfares are dominated by modern architecture, with the historic streetscape having virtually disappeared. This pattern of internal-external differentiation aligns with the historical evolution of the neighborhood—the outer arterial roads underwent large-scale reconstruction, significantly disrupting the original fabric, while the internal alleys, due to limited accessibility, allowed for the relatively complete preservation of historic buildings.

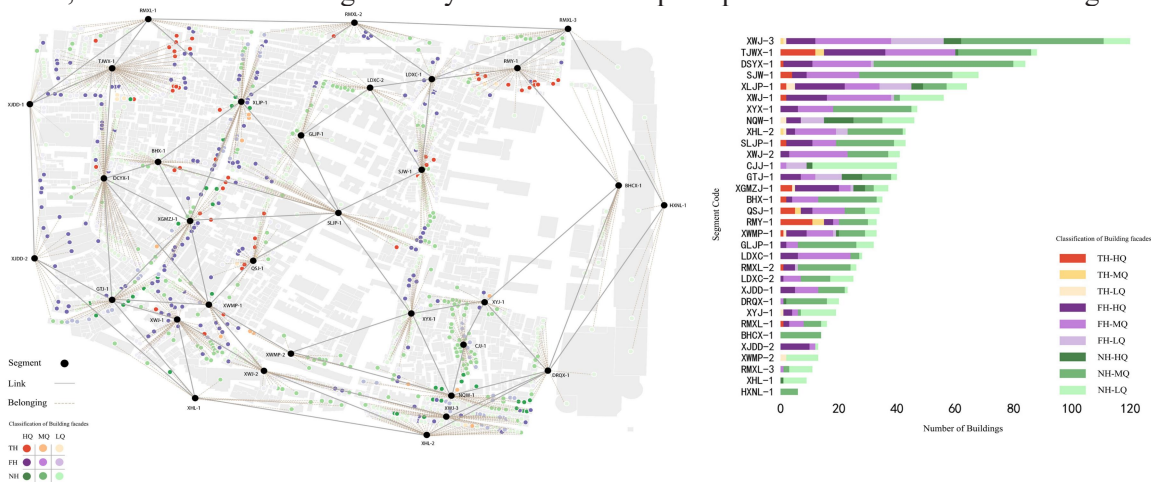


Figure 3. Classification and Spatial Distribution of Building Facades

High-quality sections are concentrated along the historic core axis, including Tangjiawan Alley (1.000), the first section of Xiuwen Street (0.935), and Xugongmen Zhengjie (0.834). Moderate-quality areas are located in the central transitional zone, such as Gutan Street (0.458) and Quansiji (0.534), where historic and newer buildings coexist. Low-quality sections dominate the periphery along major roads like Huangxing South Road (0.000) and Xihu Road Section 1 (0.008), lowering the overall quality of the streetscape. Notably, Section 2 of Xiwen Miaoping (0.093) in the core area features low-quality buildings despite its high historical value, making it a priority for renewal.

4.2 Perceptual Characteristics of Spatial Gravity Intensity

The spatial attraction factors across different sections of the neighborhood exhibit multidimensional spatial differentiation; areas with high values for each indicator do not fully overlap, and overall, a pattern emerges in which peripheral clustering coexists with internal dispersion Figure 4.

In terms of the spatial distribution of various factors, sections with high green visibility rates are primarily found along peripheral urban arterial roads, with the highest rate observed on

a section of Xiangjiang Avenue, followed by certain sections of Renmin West Road, where street tree coverage is relatively complete. Overall, green visibility rates within city blocks tend to be low, reflecting the common characteristic of insufficient green space penetration in historic districts. The overall openness of the sky is acceptable, but it is notably lower along the Shijingwan and Shanglijiapo sections. This is primarily due to obstructions from commercial shanties and narrow spacing between walls, with informal structures having a certain negative impact on the quality of the street space.

Historical and cultural POIs are scattered, mainly in Dengrenqiao Alley (5), Xiwen Miaoping, and Xuegongmen Zhengjie, with limited density and weak spatial spillover. Commercial POIs are highly concentrated along the eastern boundary, especially Huangxing South Road (69) and Dengrenqiao Alley (37), while internal coverage is sparse. Public facility POIs largely overlap commercial areas, leaving the historic core underserved. Overall, cultural resources cluster in the western inner core, while commercial and public services concentrate in the east, creating a spatial mismatch that limits the conversion of cultural assets into vitality.

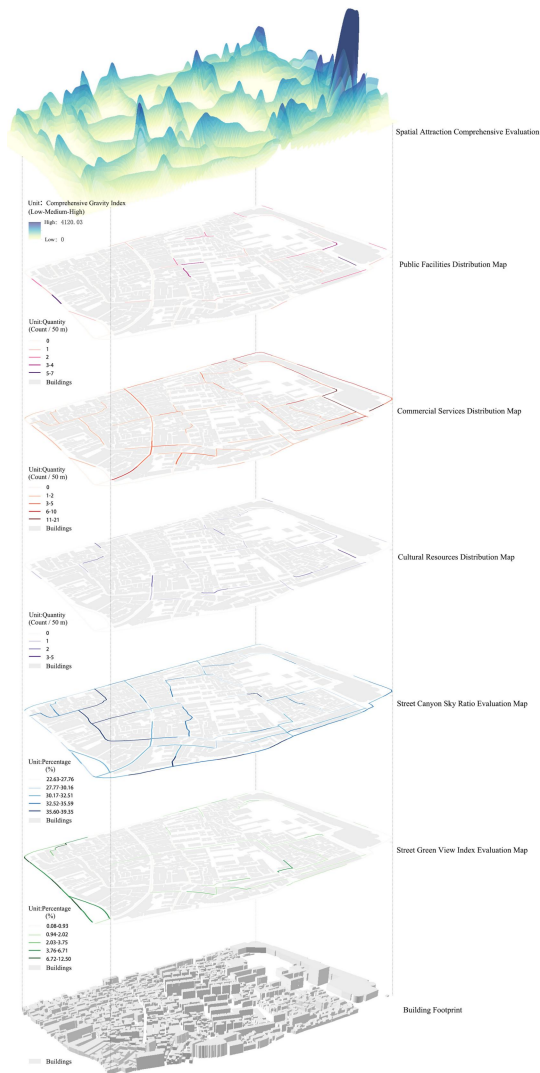


Figure 4. Spatial Distribution of Gravity Elements

4.3 Empirical Patterns of Pedestrian Activity Vitality

The pedestrian activity vitality of individual street segments broadly replicates the concentric differentiation pattern of peripheral arterials exceeding interior alleys. Normalized vitality scores reveal a high degree of spatial polarization Figure 5 and Figure 6.

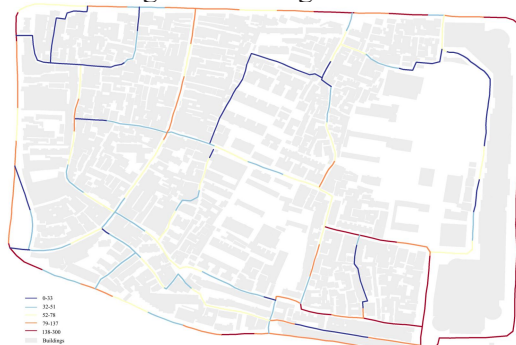


Figure 5. On-site Pedestrian Count Statistics



indicating significant spatial differentiation across segments in physical quality, spatial gravity, and pedestrian vitality. AVI exhibits the

highest dispersion, reflecting the most pronounced clustering and dispersal of pedestrian vitality.

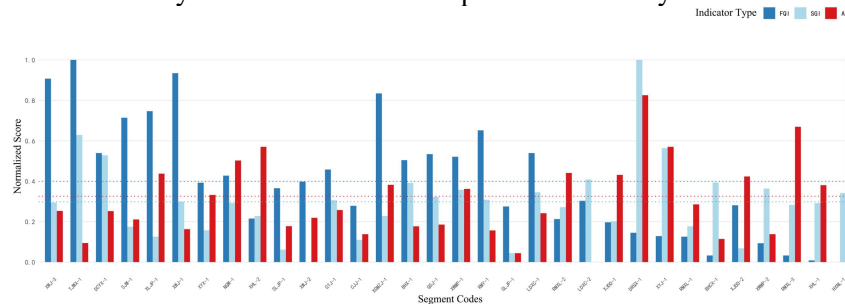


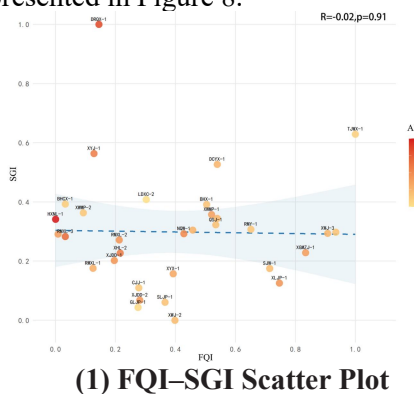
Figure 7. Normalized FQI, SGI, and AVI Score Distribution

FQI high-value segments are concentrated in TJWX-1 (1.000), XWJ-1 (0.935), and XWJ-3 (0.907)—core alleys with well-preserved historic fabric—while low-value segments are represented by HXNL-1 (0.000) and XHL-1 (0.008), peripheral segments dominated by modern construction. SGI peaks at DRQX-1 (1.000), followed by TJWX-1 (0.629) and XYJ-1 (0.564), which concentrate cultural resources; XWJ-2 (0.000) and GLJP-1 (0.044) exhibit the weakest gravity due to functional impoverishment. AVI high-value segments are concentrated in HXNL-1 (1.000), DRQX-1 (0.825), and RMXL-3 (0.669)—major circulation corridors and commercial nodes—while LDXC-2 (0.000) and GLJP-1 (0.043) record near-zero vitality.

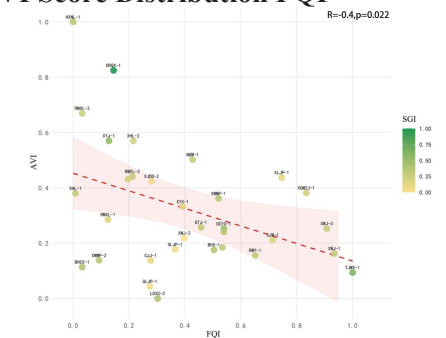
A pronounced spatial misalignment is evident between FQI and AVI high-value segments: the mean AVI of the top five FQI segments is only 0.266, while the mean FQI of the top five AVI segments is only 0.164. The two groups exhibit virtually no overlap, providing preliminary evidence of a structural divergence between physical quality and pedestrian vitality.

4.4.2 Spearman correlation analysis between dimensions

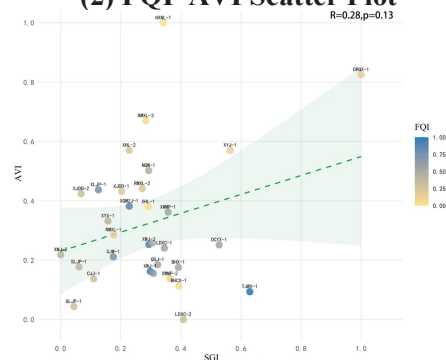
Results of the Spearman rank correlation tests for all three pairwise dimensional combinations are presented in Figure 8.



(1) FQI-SGI Scatter Plot



(2) FQI-AVI Scatter Plot



(3) SGI-AVI Scatter Plot

Figure 8. Scatter Plots of Correlations for the Three Pairwise Dimensional Combinations

FQI-SGI: $r = -0.02$, $p = 0.910$; the test is non-significant, indicating no linear association between physical facade quality and spatial gravity Figure 8-(1). The degree of traditional streetscape preservation and the strength of functional content attractiveness operate independently, exhibiting distinct spatial distribution logics at the segment level.

FQI-AVI: $r = -0.400$, $p = 0.022$; the correlation is significant at the 0.05 level, revealing a significant negative relationship Figure 8-(2). Segments with higher facade quality exhibit systematically lower pedestrian vitality, indicating a structural divergence between physical conservation and vitality activation. This "high quality-low vitality" misalignment is attributable to the concentration of high-FQI

segments within strictly regulated historic core zones where commercial function insertion is constrained and spatial accessibility is relatively weak—reflecting the absence of effective coordination between the physical conservation orientation and vitality activation demands in current historic district management.

SGI–AVI: $r = 0.280$, $p = 0.130$; the positive trend, while not statistically significant at the 0.05 level, suggests that segments with stronger spatial gravity tend to exhibit marginally higher pedestrian vitality Figure 8-(3). The richness of functional content and the quality of spatial form perception exert a certain facilitative effect on pedestrian aggregation, though this effect is not yet statistically robust, indicating that the conversion of gravity into vitality is subject to interference and constraint from additional factors.

Synthesizing the three correlation results, the three dimensions do not exhibit simple linear transmission relationships. The significant negative correlation between FQI and AVI is the only statistically confirmed result among the three pairs, indicating that under the current conservation management framework,

Table 4. Classification of Street Segment Coupling Typologies and Indicator Means

Coupling Typology	Segment Codes	Mean FQI	Mean SGI	Mean AVI
Type I — Quality-Dominant, Vitality-Lagging	TJWX-1, XWJ-1, XWJ-3, XGMZJ-1, SJW-1, RMY-1, DCYX-1, BHX-1, QSJ-1	0.735	0.353	0.208
Type II — Gravity–Vitality Synergistic	DRQX-1, XYJ-1, NQW-1, XHL-2	0.389	0.521	0.617
Type III — Vitality-Dominant, Quality-Deficient	HXNL-1, RMXL-3, XHL-1, XLJP-1, RMXL-2, XJDD-1	0.199	0.253	0.560
Type IV — Comprehensively Low-Value, Latent Potential	XYX-1, SLJP-1, XWJ-2, GTJ-1, CJJ-1, XWMP-1, GLJP-1, LDXC-1, LDXC-2, XJDD-2, XWMP-2, RMXL-1, BHCX-1	0.312	0.214	0.210

4.5.2 Characterization of each coupling typology
The three-dimensional mean profiles for each coupling typology are presented in Figure 9, with specific characteristics as follows.

Type I — Quality-Dominant, Vitality-Lagging (9 segments), including TJWX-1, XWJ-1, and XWJ-3. Mean FQI of 0.735 substantially exceeds the full-sample mean, while mean AVI is only 0.208. Streetscape preservation is excellent, but commercial functions are constrained by conservation regulations, producing a pronounced gap between physical quality and spatial vitality.

Type II — Gravity–Vitality Synergistic (4 segments), including DRQX-1, XYJ-1, NQW-1, and XHL-2. Mean SGI of 0.521 and mean AVI of 0.617 both significantly exceed the full-sample mean, while mean FQI is only 0.389. Functional content is rich and pedestrian vitality

improvements in physical quality not only fail to automatically translate into vitality gains but may in fact exert a suppressive effect. This finding underscores the need for historic district renewal practice to transcend a purely physical conservation logic, and validates the necessity of constructing a three-dimensional assessment framework to identify segment coupling typologies—providing a quantitative basis for the formulation of differentiated renewal strategies.

4.5 Identification of Street Segment Coupling Typologies and Spatial Patterns

4.5.1 Clustering method and determination of optimal typology number

Using the normalized FQI, SGI, and AVI scores of 32 street segments as input variables, K-means clustering was applied to classify coupling typologies (Table 4). Jointly applying the elbow method and silhouette coefficient, the silhouette coefficient reached its peak at $k = 4$, at which point the SSE curve exhibited a pronounced inflection point. Accordingly, the 32 segments were classified into four coupling typologies.

is high, but facade preservation is poor; streetscape coordination represents the primary renewal direction.

Type III — Vitality-Dominant, Quality-Deficient (6 segments), including HXNL-1, RMXL-3, and XHL-1. Mean AVI of 0.560, mean FQI of 0.199. Pedestrian vitality is sustained primarily by locational accessibility and commercial agglomeration rather than physical quality; the renewal priority is to progressively improve streetscape quality while maintaining existing vitality.

Type IV — Comprehensively Low-Value, Latent Potential (13 segments), including XYX-1, GLJP-1, and LDXC-2. All three indicators fall below the full-sample mean. This typology accounts for the largest number of segments (40.6%), characterized by monotonous functional programming and weak accessibility.

These segments represent the most comprehensively deteriorated group within the district and require priority investment in cultural function supplementation and infrastructure provision.

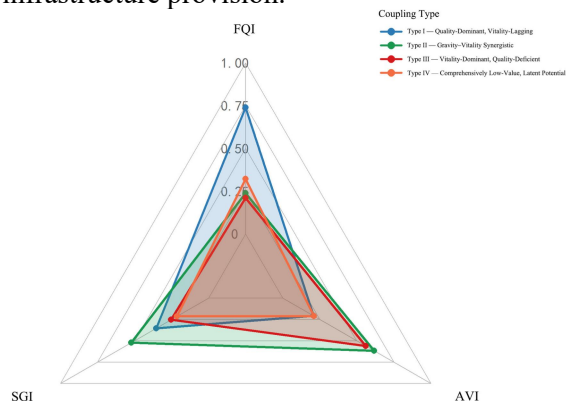


Figure 9. Radar Chart of Three-Dimensional Indicator Scores for Each Coupling Typology

5. Discussion

5.1 Structural Divergence between Physical Quality and Vitality, and the Gravity Conversion Mechanism

The significant negative correlation between FQI and AVI ($r = -0.400$, $p = 0.022$) reveals a structural "high quality–low vitality" divergence attributable to multiple compounding factors. High-FQI segments are predominantly located within strictly regulated conservation core zones, where commercial function insertion is severely constrained and functional attractiveness for external visitors is limited. These segments are also typically narrow interior alleys with weak network connectivity, making it difficult to sustain stable pedestrian flows. Additionally, AVI data were collected on weekdays between 16:00 and 19:00, capturing primarily quotidian residential flows, which may underestimate the latent vitality of high-quality segments during holidays and weekends.

The positive trend between SGI and AVI ($r = 0.280$, $p = 0.130$), while not statistically significant, is corroborated by Type II segments, which demonstrate that functional content richness facilitates pedestrian aggregation. The pronounced spatial misalignment between cultural–historical POIs and commercial–service POIs substantially constrains the conversion of cultural resources into realized vitality. The fact that Type II segments achieve gravity–vitality synergy is precisely attributable to the spatial co-location of these two functional categories,

confirming the pivotal role of cultural–commercial composite functions in vitality activation. The high check-in frequency of 137 instances recorded for Xiwenmiaoping Section 1, despite relatively limited empirical pedestrian counts, highlights the necessity of cross-validating social media heat data against empirically measured behavioral data. The absence of significant correlation between FQI and SGI ($r = -0.002$, $p = 0.910$) indicates that physical conservation and functional activation have yet to achieve effective spatial coordination, and that functional content programming requires independent planning intervention.

5.2 Spatial Logic of the Four Coupling Typologies and Differentiated Renewal Strategies

Given the structural differences among the four coupling typologies, renewal strategies should be calibrated accordingly. Type I segments should, within the constraints of heritage conservation, introduce lightweight commercial programs aligned with cultural–historical themes while improving internal network accessibility, thereby converting latent cultural attractiveness into realized pedestrian flows. Type II segments have already achieved a well-functioning cultural–commercial composite, making interface remediation and streetscape coordination the near-term priority. Type III segments should prioritize incremental interface improvement, progressively enhancing streetscape quality while preserving existing commercial vitality, and avoiding large-scale redevelopment that could disrupt the vitality ecosystem. Type IV segments, which constitute the largest group (13 segments, 40.6%), require priority investment in cultural function supplementation and infrastructure provision, with the gradual construction of functional linkages to the historic core, so as to prevent these segments from becoming trapped in a self-reinforcing cycle of low-quality, low-vitality decline.

5.3 Limitations

Both street-view imagery and empirical pedestrian count data were collected at a single time point, failing to capture temporal dynamics; future research should incorporate multi-period continuous monitoring. Regarding behavioral layer measurement, YOLOv8 exhibits an approximately 20% detection error rate in high-

density scenes, and social media check-in data are subject to platform and user biases that limit representativeness. Furthermore, the use of street segments as the basic spatial unit obscures intra-segment spatial heterogeneity; subsequent studies may refine the spatial unit to improve analytical precision.

6. Conclusions

Taking the Xiwenmiaoping Historic District in Changsha as the study area, this research constructs a three-dimensional comprehensive assessment framework encompassing facade quality (FQI), spatial gravity (SGI), and activity vitality (AVI), systematically quantifies 32 street segments, and identifies four spatial coupling typologies. The findings are as follows. First, the significant negative correlation between FQI and AVI reveals a "conservation paradox" in which physical preservation and vitality activation operate in structural opposition. Second, the spatial misalignment between cultural–historical POIs and commercial–service POIs constitutes the key structural constraint on district-wide vitality, and the spatial co-location of cultural and commercial functions is the critical condition for converting gravity into realized vitality. Third, a substantial conversion loss exists between social media check-in heat and physical pedestrian flows, indicating that online visibility cannot be equated with spatial vitality. Among the four coupling typologies, the comprehensively low-value, latent-potential type accounts for the highest proportion of segments and represents the primary constraint on overall district vitality improvement.

These findings indicate that vitality enhancement in historic districts must transcend a purely physical conservation logic, and that functional activation and accessibility improvement must be pursued in coordination within the conservation framework. Segments characterized by well-preserved streetscapes but lagging vitality should be activated through the introduction of lightweight cultural programs and improvements to wayfinding accessibility. Comprehensively low-value segments require cultural function supplementation and infrastructure investment to establish functional linkages with the historic core and arrest the deepening of intra-district spatial polarization. The multi-dimensional quantitative framework developed in this study demonstrates strong methodological transferability and can be

extended in future research toward temporal dynamic monitoring and multi-city comparative analysis.

References

- [1] Li, C.R., Li, Y.X., Xu, M., et al. Research on the cognition of value characteristics of historical and cultural cities from the perspective of holistic conservation: A case study of Huangshan City, Anhui Province. *China Ancient City*. 2025; 39(04): 55-61.
- [2] Du, J., Miao, C.H., Xu, J.W., et al. Research on evaluation and improvement paths of historic district renewal under the background of cultural-tourism integration: A case study of three historic districts in Kaifeng. *Journal of Natural Resources*. 2025; 40(01): 164-180.
- [3] Wan, X., Sun, H.J., Xu, N., et al. Value symbiosis-driven mechanism of participatory renewal in historical and cultural districts: A case study of Nanjing Old South City. *Journal of Natural Resources*. 2025; 40(10): 2652-2667.
- [4] Xue, P.T., Zheng, J.M., Chen, Y.S., et al. Satisfaction study of historical and cultural districts from the perspectives of tourists and residents: A case study of Xinghua Prefecture Historical and Cultural District in Putian. *Journal of Xingtai University*. 2026; 41(01): 81-91.
- [5] Fu, Y., Lai, H.B. Research on satisfaction evaluation model of wayfinding systems in Zhongshan Road Historical and Cultural District, Shenyang based on PCA-AHP. *Architecture & Culture*. 2026; (02): 183-185.
- [6] Gu, Y., Quintana, M., Liang, X., et al. Designing effective image-based surveys for urban visual perception. *Landscape and Urban Planning*. 2025; 260: 105368.
- [7] Ye, Z.Y., Zhu, J.W., Wang, J.C., et al. Research on improving pedestrian environments based on self-collected street view images and deep learning: A case study of Changsha. *South Architecture*. 2026; (02): 30-40.
- [8] Qian, C.Y., Xiao, Y., Zhou, Y. Research on perceptual measurement and spatial distribution characteristics of living streets around historic districts based on machine learning. *Chinese Landscape Architecture*. 2025; 41(11): 61-68.
- [9] Chen, X.W., Zhu, J.M., Liu, Y.C. Evaluation method and validation of street

- spatial quality in historical and cultural districts based on self-collected street view data. *Journal of Geo-information Science*. 2025; 27(11): 2770-2787.
- [10] Zheng, Y., Yang, J.Y. Research on refined urban regeneration methods based on artificial intelligence analysis of large-scale street view images. *Chinese Landscape Architecture*. 2020; 36(08): 73-77.
- [11] Liang, X., Chang, J.H., Gao, S., et al. Evaluating human perception of building exteriors using street view imagery. *Building and Environment*. 2024; 263: 111875.
- [12] Ahmed, R.J., Jamal, H.H. Urban visual characteristics and livability of heritage areas: A case of Erbil's Qaysari Bazaar. *Sulaimani Journal for Engineering Sciences*. 2026; 12(2).
- [13] Wang, M., Zhou, X., Chen, Y. A comprehensive survey of crowd density estimation and counting. *IET Image Processing*. 2025; 19(1): e13328.
- [14] Zhao, P.F., Chen, G., Zhao, J.L., et al. Tourist perception of Grand Canal historical and cultural districts based on UGC data. *Urban Development Studies*. 2025; 32(10): 24-30+37.
- [15] Wang, H.Y., Che, X.H., Xu, X.C., Xu, S.H., Li, H.S. Green visible index extraction and analysis of street view image using DeepLabv3+ model: Taking within the Third Ring Road in Beijing as an example. *Bulletin of Surveying and Mapping*. 2024; (3): 88.
- [16] Xu, C.F., Li, M., Hu, Y.K., et al. Scenic beauty assessment and spatiotemporal driving mechanisms of Nanjing urban areas based on street view images. *Journal of Chinese Urban Forestry*. 2025; 23(04): 61-71.
- [17] Gong, H., Li, T., Wang, L., et al. An improved YOLOv8-based dense pedestrian detection method with multi-scale fusion and linear spatial attention. *Applied Sciences*. 2025; 15(10): 5518.
- [18] Shen, S.Y., Gu, G.X., Zhang, Y., et al. Research on facility spatial structure of five new towns in Shanghai based on POI data. *Scientia Geographica Sinica*. 2024; 44(05): 843-852.
- [19] Gou, F., Chen, Z., Yang, X., et al. Spatiotemporal and sentiment analysis of tourist sources in distinctive pedestrian street using social media data. *Applied Spatial Analysis and Policy*. 2025; 18(3): 97.
- [20] Chen, X., Sun, Y., Ibrahim, F.I.B., et al. Social media interaction and built environment effects on urban walking experience: A machine learning analysis of Shanghai Citywalk. *PLOS ONE*. 2025; 20(4): e0320951.
- [21] Huang, K., Kang, P., Zhao, Y. Quantitative research of street interface morphology in urban historic districts: A case study of West Street Historic District, Quanzhou. *Heritage Science*. 2024; 12(1): 1-27.
- [22] Rui, J., Xu, Y., Li, X. Destigmatizing urban villages by examining their attractiveness: Quantification evidence from Shenzhen. *Habitat International*. 2024; 150: 103120.
- [23] Liao, W., Liu, P.A., Chen, Z., et al. Investigating impacts of renovated exteriors in historic districts on visitor vitality through space syntax reflection. *npj Heritage Science*. 2025; 13(1): 336.
- [24] Gong, C., Hu, C., Ding, M., et al. Embodied perception of alleyways in mountain city historic districts: Perspectives of young and older adults in Chongqing Ciqikou. *Frontiers in Psychology*. 2026; 17: 1714333.
- [25] Guo, H.J., Zhong, Y.J., Xing, H.F., et al. Urban street spatial classification method integrating taxi trajectories and street view images. *Tropical Geography*. 2024; 44(05): 906-920.